ISSN 0029-3865

CBPF-NF-084/83

APPLICATIONS OF MÖSSBAUER SPECTROSCOPY IN THE STUDY OF MINERALS: SOME RECENT TRENDS*

by

J. Danon

Centro Brasileiro de Pesquisas Físicas - CNPq/CBPF
Rua Dr. Xavier Sigaud, 150
22290 - Rio de Janeiro, RJ - Brasil

*Invited lecture - International Conference on Mössbauer Effect Alma-Ata, Soviet Union, October 1983.

The recent development of physics and chemistry of solids towards the study of multiphase systems arises as a consequence of the improvements in analytical techniques such as electron microscopy, microprobe analysis, X-ray diffraction and in the field of Mössbauer Spectroscopy by the sophistication in the analysis of complex spectra using computer methods.

Such improvements have led in the field of mineralogy to the development of studies in structural, electrical and magnetic properties of minerals and natural solid solutions to the point that a new interdisciplinary domain, the physics of minerals, is becoming a firmly established research area.

We have selected three examples of such studies in which Mössbauer spectroscopy is playing a determinant role: magnetic order in silicates, biomineralization of iron by bacteria and order-disorder transitions in Fe-Ni alloys in meteorites.

1. Magnetic Order in Silicates

Silicates provide an area for application of the well-established ideas of magnetism in insulating 3d compounds, particularly in quasi-one or two dimensional compounds.

Mössbauer spectroscopy has contributed substantially over the last few years to an understanding of the magnetism of a number of silicates with sheet and chain structures[1,2]. Magnetic ordering is now known to occur for a wide variety of iron-rich silicate minerals below tempera-

tures in the range 1-100K although none have yet been discovered that are ordered at room temperature. Table 1 lists Néel temperatures found for silicates. References to work on their magnetic properties are given in (1,2).The ordering somehow turns out to be antiferromagnetic in every case but there are remarkable variations which reflect the arrangements of octahedral sites where the iron is normally located.

Framework silicates the most widespread rock-forming minerals (quartz, feldspar) contain too little iron for continuous percolation paths to exist among ferrous or ferric cations, and therefore do not order magnetically. Iron-rich sheet silicates, however, show very interesting collective magnetic behaviour. The structures of the two main families are illustrated in figure 1. 1:1 layer silicates known to order include the trioctahedral, ferrous serpentine minerals greenalite and berthiérine and mixed-valent cronstedtite[3]. Some magnetic hyperfine spectra at 4.2K are shown on figure 2. The ferrous absorption is rather similar for all layer silicates, and it is well fitted with an axial negative, electric field gradient ($V_{zz} \sim -3$mm/s,$\eta=0$) with an angle $\theta \sim 90º$ between the field gradient z-axis and the direction of the magnetic hyperfine field. These values imply that the iron lies in sites where the ligand octahedron is effectively trigonally distorted in such a way that the orbital singlet state $^5A_{1g}$, $\ell_z=0$ is lowest in energy[4]. When spin-orbit coupling is taken into account, the spin Hamiltonian is of the form DS_z^2, with D positive, so the z-axis is the hard magnetic direction and the moments tend to lie in the plane perpendicular to z. Hence $\theta \cong 90º$. Values of D in sheet silicates are $\sim$10K, and the trigonal splitting of the cubic T_{2g} triplet level is 1000-2000K. By analogy with $Fe(OH)_2$ whose structure resembles that of the octahedral sheet, it was suggested that the z axis coincides with the c' direction, normal to the sheets.

The dominant exchange interactions in greenalite

and other sheet and chain silicates containing ferrous iron or a mixture of ferrous and ferric iron on octahedral sites turn out to be ferromagnetic, as expected for Fe^{2+}-O-Fe^{2+} superexchange paths with a bond angle near 90º Curie-Weiss temperatures θ_p, are always positive, thus ferromagnetic units are the characteristic element in their magnetic order. For layer silicates, it is the octahedral sheets which are ferromagnetic, with the moments lying essentially within the plane of the sheet. Exchange coupling between the sheets is weak, but antiferromagnetic. Hence there is a large peak in the low-field susceptibility at the ordering temperature T_N and an upturn in the magnetization of ferrous sheet silicates below T_N in fields $\geq$1 kOe due to a spin flop transition. These minerals could easily be mistaken for ferromagnets from their hysteresis loops but the magnetic order in zero field actually consists of ferromagnetic sheets alternately ordered in opposite directions because of the weak antiferromagnetic interplane interactions, as shown in figure 3. This was demonstrated by neutron diffraction, which shows a series of extra magnetic reflections with indices (h,h,(m+1)/2) appearing below T_N. The ratio of intraplane to the interplane coupling is of order 50, so these materials are magnetically as well as crystallographically two-dimensional.

Mössbauer spectra and magnetic order in trioctahedral 2:1 layer silicates such as Miniesotaite (a ferrous talc) resemble those of their 1:1 counterparts. The origin of ferromagnetic coupling within the planes is again the near -90º Fe^{2+}-O-Fe^{2+} superexchange bond angle, which leads to values of the exchange constant of =2K. There is evidence that the Fe^{2+}-O-Fe^{3+} interaction is also positive, and this may be due to virtual electron transfer, the double exchange interaction. It is generally expected that the exchange should be positive whenever electron hopping occurs. By contrast, the purely ferric, dioctahedral sheet silicates have different magnetic structures. Examples are oxidized, ferric cronstedtite, ferripyrophyllite and nontronite.There

the dominant interactions are antiferromagnetic Fe^{3+}-O-Fe^{3+} superexchange coupling within the plane, leading to negative values of θ_p.

The contrast between the latter two minerals provides a nice example of the frustation effect of antiferromagnetic interactions on a disordered lattice. The concept of frustration[5] was introduced by Anderson and Toulouse in relation to the spin glass problem, but it has widespread validity in magnetism of disordered and amorphous systems. Bonnin[6] has pointed out its relevance to dioctahedral sheet silicates. Figure 4a shows the honeycomb structure when only M2 sites in the octahedral layer are occupied. Antiferromagnetic nearest-neighbour interactions can all be simultaneously satisfied around the six-membered rings and perfect antiferromagnetic order can be established in principle. However, if the site occupancy is random (figure 4b), there will appear three-membered rings where antiferromagnetic interactions cannot be simultaneously satisfied and Coey finds that random non-collinear (speromagnetic) order sets in at a temperature which is much lower than that expected from the strength of the individual superexchange bonds[2]. Ferripyrophyllite, a new mineral discovered by F.V. Chukhrov in 1978, is the ferric form of pyrophyllite, the uncharged 2:1 doctahedral end member. The ideal formula is

$$\text{Ferripyrophillite: } Fe_2^{3+}[Si_4]O_{10}(OH)_2$$

Nontronite is a fairly common ferric smectite with a small net charge, compensated by interlayer cations in the ideal formula, the octahedral layer is also saturated with ferric iron which occupies 2/3 of the available sites

$$\text{Nontronite: } \langle M^+ \rangle \{Fe_2^{3+}\}[Si_4]O_{10}(OH)_2$$

The ordering temperatures of the two minerals, 18K and 2K respectively, differ by almost an order of magnitude.

They are expected to be quite sensitive to whether or not the ferric cations are spatially ordered on M2 sites within the trioctahedral sheet. Cation order of Fe^{3+} on M2 sites has been inferred from the paramagnetic Mössbauer spectrum of ferripyrophillite, essentially a single unresolved doublet by Coey and Chukhrov[7]. This gives a honeycomb magnetic lattice which has a relatively high magnetic ordering temperature. However cation disordered due to random occupation of 2/3 of M1 and M2 sites gives a triangular lattice with random vacancies, and the antiferromagnetic interactions are frustrated by three membered rings leading to the very low magnetic ordering temperatures found by Bonnin in nontronite.

Chain silicates resemble the 2:1 layer silicates structurally in that the ribbons can be considered as strips of the 2:1 layers. Inner octahedral sites (M1 in pyroxenes, M1-M3 in amphiboles) should therefore resemble the sites in the octahedral sheet to some extent, and this expectation is borne out by the sign and magnitudes of $1/2\ e^2qQ$. Splitting of the T_{2g} triplet deduced from the temperature dependence of Δ is small in orthoferrosilite and $n \cong 1$, so the trigonal model does not apply. However η is small for M1 and M3 sites in crocidolite, and the magnetic structure of this alkali amphibole asbestos has been shown by neutron diffraction to consist of ferromagnetic ribbons, coupled antiferromagnetically as sketched in figure 5. Grunerite probably has a similar magnetic structure, and the spin flop in both minerals occurs in 15 kOe at 4.2K. Magnetic ordering has also been reported for riebeckite, crossite and arfvedsonite. Antiferromagnetic coupling is stronger in chain silicates than sheet silicates on account of the shorter distance between the ferromagnetic units.

Among the group silicates, the magnetic order in fayalite has been studied by susceptibility measurements, Möss-

bauer spectroscopy[8] and neutron diffraction. Antiferromagnetism sets in below 66K, and the proposed magnetic structure is canted like that of haematite, down to 20K. A second transition to a collinear antiferromagnetic structure below 20K is postulated. There have also been reports of magnetic ordering from low-temperature Mössbauer spectra of the iron-rich minerals ilvaite staurolite, laihunite (a partially ferric form of olivine) and almandite garnet, but there is insufficient data at present to determine the magnetic structures of these minerals[1].

Because of the chemical variability of minerals and the rarity of true iron end-members of solid solution series, some variation in the ordering temperatures and other magnetic parameters is inevitable. A Mössbauer study of the low temperature spectra of olivines $Mg_{2-x}Fe_x[Si]O_4$ as a function of x has shown that magnetic relaxation effects are important for intermediate members of the series[9]. The spectra for a sample with x=0.4, have been successfully interpreted in terms of superparamagnetic fluctuations of small groups of ferrous ions some 20 Å in size. Best fits were obtained with a distribution of relaxation times at a given temperature corresponding to a distribution of cluster sizes. It was found that natural olivines from igneous intrusions have a tighter and less asymmetric size distribution than synthetic olivines, due to the difference in cooling rates. Magnesium-rich olivines with x=0.34 from recent lavas were also found to order magnetically around 5K.

Study of magnetic order in silicate minerals is in its early stages. Magnetic hyperfine spectra contain much more information, particularly concerning the electronic structure of the ferrous ion, than is available from paramagnetic quadrupole doublets. Spectra which are unresolved in the paramagnetic state may be clearly separated below the magnetic ordering temperature. However, for a complete account of the magnetic properties of the silicates the Mössbauer spectra must usually be interpreted in conjunct-

ion with magnetization, susceptibility and neutron diffraction data.

2. Biomineralization of iron by bacteria

Biomineralization phenomena have recently been object of intense investigations, due its theoretical significance to geochemistry and its great practical importance in ore mineralogy. A most interesting exemple, intimately connected with the problems of the orientation of organisms in the earth magnetic field, is that of magnetotactic bacteria Mössbauer spectroscopy has been used as a basic tool for the elucidation of the iron biomineralization in these microorganisms.

In the freshwater magnetotactic spirillum, Aquaspirillum magnetotacticum, iron comprises 2% or more of the cellular dry weight[10]. Electron microscopy studies of this organisms show that it contains Fe_3O_4 particles, which are cuboidal, 40-50 nm in width, and are arranged in a chain that longitudinally traverses the cell. The particles are enveloped by electron-transparent and electron-dense layers; a particle and its enveloping membrane has been termed a magnetosome[11].

The magnetosomes impart a magnetic dipole moment to the cell, parallel to the axis of mobility[12]. According to the passive orientation hypothesis[13], the cell is oriented as it swims in the geomagnetic field by the torque exerted on the magnetic dipole moment by the field. Cells are either North-seeking or South-seeking, that is, they either swim in the field direction or opposite to the field direction[14]. The virtual component of the geomagnetic field selects the predominant polarity in natural environments by directing and keeping bacteria away from the oxygen-rich surface waters and in the sediments[15,16,17].

Since A. magnetotacticum is cultured in a chemically defined medium in which iron is available as soluble fer-

ric quinate the presence of intracellular Fe_3O_4 implies a process of bacterial precipitation of this mineral, with control of particle size, number and location in the cell.

In order to elucidate the Fe_3O_4 biomineralization process, cells and cell fractions, some isotopically enriched in Fe-57, have been studied by Mössbauer spectroscopy[18]. Cells of a non-magnetotactic variant that accumulated iron but did not make Fe_3O_4 and of a cloned, nonmagnetotactic strain that accumulated less iron, were also studied. The results suggest that Fe_3O_4 is precipitated by reduction of a hydrous ferric-oxide precursor.

Mössbauer spectra of wet packed cells enriched in Fe-57 at 200K can be analyzed as a superposition of spectra corresponding to Fe_3O_4 (Fig. 6A) a broadened quadrupole doublet with parameters characteristic of ferric iron (Fig.6B), and a weak quadrupole doublet with parameters corresponding to ferrous iron (Fig. 6C).

Figure 6B was also observed in lyophilized cells and has isomer shift and quadrupole splitting parameters similar to iron in ferritin and in the mineral ferrihydrite, indicative of ferric iron with oxygen coordination. The relative intensity of B to A was somewhat variable from sample to sample, depending on growth conditions. At 80K, spectrum A corresponds to Fe_3O_4 below the Verwey transition and the parameters of spectrum B and the relative intensity of B to A are relatively unchanged compared to the spectrum at 250K. Between 80 and 4.2K, however, the intensity of B decreased with decreasing temperature so that at 4.2K only a residual doublet remained. A similar temperature dependence for spectrum B was also obtained in lyophilized cells.

The isomer shift and quadrupole splitting parameters of spectrum C correspond to high spin ferrous iron in coordination with oxygen or nitrogen. This spectrum was not observed with lyophilized cells, possibly as a result of oxidation during sample preparation. Wet, packed cells kept unfrozen under anaerobic conditions contained increased

amounts of material responsible for spectrum C and correspondingly less material with spectral characteristics B. Thawing and aeration of these frozen cells resulted in increases in B spectral lines and concommitant decreases in C spectral lines. This indicates that the iron atoms responsible for spectrum C came from reduction of the iron atoms giving spectrum B. Unlike that of spectrum B, the intensity of spectrum C did not decrease between 80 and 4.2K.

The decrease in the intensity of spectrum B between 80 and 4.2K can be explained as the onset of magnetic hyperfine interactions at low temperature resulting in a concommitant decrease in the intensity of the central absorption doublet. This phenomenon has been observed with Mössbauer spectroscopy of ferritin[19].

For T 80K, the spectrum of lyophilized non-magnetotactic cells consisted primarily of the quadrupole doublet characteristic of ferric iron (spectrum B). Below 80K, the intensity of the quadrupole doublet decreased with decreasing temperature while the intensity of a six-line spectrum flanking the doublet increased. At 4.2K the spectrum (Fig. 7) consisted primarily of the six broadened magnetic hyperfine lines, with a small residual doublet in the center. Application of a longitudinal magnetic field of 60 kOe produced broadening of the six-line spectrum but with no appreciable shifts in the line positions and no decreases in any line intensities.

These spectral characteristics are indicative of small particles of hydrous-ferric-oxide with antiferromagnetic exchange interactions similar to those of the ferric iron within ferritin micelles and in ferrihydrite. By comparison with ferritin, the experimental results indicate that hydrous-ferric-oxide particles in the non-magnetotactic cells are of the order of 100 Å in diameter, or less. Unlike ferritin or ferrihydrite, however, there was a residual quadrupole doublet in the 4.2K spectrum of magnetotactic and non-magnetotactic cells. The intensity of this residual doublet va

ried somewhat from sample to sample, but its presence suggests another high spin ferric material with high temperature spectral characteristics similar to those of ferrihydrite, but with iron atoms less densely packed so that magnetic exchange interactions between them are weaker and the spectrum is not magnetically split at 4.2K. This latter material was also observed in a cloned, nonmagnetotactic strain of A. Magnetotacticum that accumulates less iron.

The Mössbauer spectrum of wet, packed cells of the cloned non-magnetotactic strain consisted of a quadrupole absorption doublet for $T \geq 4.2K$. The spectral parameters(Fig.8). obtained at 80K were similar to those of spectrum 6B in magnetotactic cells[6] indicating the presence of a high spin ferric iron material. Application of an external 60 kOe magnetic field at 4.2K results in spectra with a broad distribution of hyperfine fields. These spectral characteristics indicate the presence of high spin Fe^{3+} in a hydrous oxide with magnetic exchange interactions <4K, that is, where the iron atoms are less densely packed than in ferrihydrite. This material has similar spectral characteristics to the iron storage material in E. coli[20].

When these wet, packed cells were held above 275K in an anaerobic environment, a ferrous spectrum similar to spectrum 6C appeared, in addition to the ferric-iron doublet. This indicates that the hydrous-ferric-oxide in cells of this strain can be reduced to ferrous iron as with cells of the other strain.

On the basis of the foregoing results it has been proposed that A. Magnetotacticum precipitates Fe_3O_4 in the sequence: Fe^{3+} quinate $\rightarrow Fe^{2+} \rightarrow$ low density hydrous ferric $\rightarrow$ oxide $\rightarrow$ ferrihydrite $\rightarrow Fe_3O_4$[18]. In non-magnetotactic cells the process stops with ferrihydrite. In cells of the cloned, non-magnetotactic strain the process stops with low density hydrous ferric oxide.

In the proposed process, iron enters the cell as Fe^{3+} chelated by quinic acid. Reduction to Fe^{2+} releases iron from the chelator. Fe^{2+} is reoxidized and accumulated as

the low density hydrous iron oxide. By analogy with the deposition of iron in the micellar cores of the protein ferritin[21] this oxidation step might involve molecular oxygen, which is required for Fe_3O_4 precipitation in A. Magnetotacticum. Dehydration of the low-density hydrous ferric oxide results in ferrihydrite. Finally, partial reduction of ferrihydrite and further dehydration yields Fe_3O_4.

In addition to elucidating the Fe_3O_4 precipitation process, Mössbauer spectroscopy has been used to determine the effective viscosity of the magnetosomes in magnetotactic cells[22].

The detection is based on the fact that in cells at ambient temperatures the magnetosomes will undergo small diffusive displacements, the magnitudes of which are related to the viscosity of their surroundings. It has been previously shown that for iron containing colloidal particles introduced into a viscous fluid, the Mössbauer line width is inversely proportional to the viscosity of the fluid[23]. Furthermore, it has been demonstrated recently that the Mössbauer effect (ME) on iron-containing proteins in cells can be used to determine the viscosity of the iron containing environment[24].

The Mössbauer spectrum of the whole magnetotactic cells at T=275K was dramatically different from that of the frozen cells (T=265K). At 275K it consisted primarily of a broad-line of width $\Gamma = 72 \pm 1$ mm/s. The width of the broad line increased with increasing temperature to $\Gamma = 139.0$ mm/s at T=295K. However, the total spectral intensity was temperature independent and equal to the total spectral intensity of the sharp line spectrum of the frozen cells.

The dramatic change of the spectral shape from a normal sharp-line spectrum between +8 and -8 mm/s to an anomalous broad-line spectrum with half width 10 cm/s can be explained by the onset of diffusive motions of the Fe_3O_4 particles in the bacteria as they are warmed through the solid liquid phase transition of the cytoplasmic fluid at 270K. Evidence for this comes from the fact that the freeze-dried

cells the sharp-line spectrum persists at 300K and the broad-line spectrum is never observed. An analysis of the broad-line spectra was based on an extention of the "bounded diffusion" model previously developed for iron-containing proteins in whole cells[24,25,26].

It was found that rotational and translational motions of the individual particles are small ($\theta < 1.5^0$; $\langle x^2 \rangle^{1/2} < 8.4$ Å) and that the effective viscosity of the cytoplasm of the magnetotactic bacteria is about 15 times greater than the viscosity of water.

3. Order-disorder transitions in Fe-Ni alloys in meteorites.

The main source of information on the cosmochemistry of the solar system are meteorites and lunar samples. One of the most important questions regarding these materials are the thermal processes which they have been subject. The cooling rate problem of meteorites is essential for the understanding of their mineralogical features[27]. This is particularly clear with the iron-nickel alloys of meteorites, which are present in most meteorites, either as a major constituent, in the so-called iron-meteorites, or in small particles as in the chondrites.

Mössbauer spectroscopy has given a fundamental contribution for the discovery of a new phase in the Fe-Ni alloys of meteorites[28,29,30], whose physical properties may be related to cooling rates and other thermal processes experienced by meteorites[31,32].

The ordered Fe-Ni (50-50) alloy forms an ordered phase with superstructure Llo at temperatures below the critical order-disorder transition of T_c=539K. Due to the extremely slow diffusion rate below this temperature it has not been possible to obtain the ordered phase by thermal annealing. In fact, the discovery of this phase has been made by neutron irradiation of the corresponding disordered

Fe-Ni alloy, which produces ordered domains of small dimensions[33,34].

The ordered phase presents a small tetragonal distortion ($\frac{c}{a}$ = 1.0036)[35] and for this reason has been called by the name of tetrataenite[36], after its discovery in meteorites.

The typical Mössbauer spectrum of meteoritical taenite presents: (Fig. 9).

a - a central single line due Fe-Ni alloy with less than about 25% Ni content.

b - a magnetic splitted hyperfine pattern, with typical assymetry due to the presence of a quadrupole splitting, which arises from the tetragonal distortion in tetrataenite.

The Mössbauer parameters of tetrataenite have been found to vary for the different meteorites[31]. Both the internal magnetic field H_i and the electrical quadrupole splitting ΔE vary with the degree of order of tetrataenite[37]. Distinct values for the ΔE have been reported, ranging from 0.25 mm/s for the Fe-Ni alloy with high degree of ordering to about $\sim$0 for the disordered alloy. The hyperfine field and the width of the absorption lines tend to increase with increasing disorder in tetrataenite.Thus, the spreading of the values of the hyperfine interactions observed reflects the different degree of ordering of tetrataenite in the different meteorites.

Fig. 10 reproduces the results obtained from Mössbauer measurements of tetrataenite extracted from iron meteorites which belong to different chemical groups of the meteorite classification. The results revealed large variations in the degree of order which were attributed to their different cooling rates below the order-disorder transition temperature.

The IA meteorites and Dayton IIID seem to have cooled slower (high degree of order in tetrataenite) than the IIIA meteorites, and the IVA meteorites like Gibeon and Harriman have a rather fast cooling rate as compared to

the previous in some meteorites, like Cratheus, the cooling rate has been fast enough that no tetrataenite has been formed.

Thus, there appears to exist an interesting correlation between the Mössbauer hyperfine parameters and the differences in cooling rates of the iron meteorites.

Besides cooling rates, other important event in the history of meteorites is shock. Shock waves can modify the degree of ordering of tetrataenite by reheating and mechanical distortions[38]. In a detailed study by Mössbauer spectroscopy of the metal particles extracted from about 20 chondrites[30], we observed a correlation between the distinct values of the hyperfine parameters and the shock history of chondrites.

On the basis of the values of the quadrupole splitting it has been possible to distinguish 3 distinct groups of chondrites. The chondrites Tieschitz, Bjurbole, Appley Bridge, Allegan, Soko Banja, S. Sēverin, Olivenza, present the value of ΔE in the range 0.25 to 0.19 mm/s ($\pm$ 0.02). For these chondrites no evidence for shock or reheating is reported from mineralogical studies. The values of the magnetic hyperfine field were found to vary around an average value of 291 kOe and the average line width Γ is 0.38 mm/s. The ordered phase appears to be in a high state of order in the metal particles of these chondrites.

Chondrites moderately shocked or with some evidence for reheating such as: L'Aigle, Dhurmsala, Parnallee, Parambu, Lake Labyrinth present the ΔE value in the range 0.16 to 0.12 mm/s. The average value for H_i is 295 kOe and for Γ is 0.45 mm/s.

For strongly reheated chondrites and with severe shock evidence such as: Ergheo, Paragould black, Paragould gray, Knyahinya, Peetz, Shaw, the value of E is practically zero or no evidence for the presence of tetrataenite is observed (Paragould and Knyahinya). The average H_i is higher (307kOe) and the lines are broadened, with average value for this group of $\sim$0.48 mm/s.

It appears thus that the degree of order of tetrataenite is influenced by several factors, such as the cooling rate, the extension of shock. Further studies are required for a detailed understanding of the correlations between the Mössbauer spectra of tetrataenite and the parameters of cosmochemical significance in meteorites.

I am indebted to J.M.D. Coey and R.B. Frankel for extended contributions to the first and second part of this paper. This work was supported by the Brazilian Academy of Sciences.

REFERENCES

1. J.M.D. Coey "Silicate Minerals" in Chemical Applications of Mössbauer Spectroscopy, G.J. Long, ed. Plenum Press, N.Y. 1983.
2. J.M.D. Coey, J. Appl. Phys. 49, 1646 (1978).
3. J.M.D. Coey, O. Ballet, A. Moukarika and J.L.Soubeyroux, Phys. Chem. Minerals 7, 141 (1981).
4. J. Varret, J. Physique 37, 6 (1976).
5. G. Toulouse, J. Vannimenus, La Recherche 8, 919 (1976).
6. D. Bonnin, Thesis, Université de Paris VI, 1981.
7. J.M.D. Coey, F.V. Chukhrov, to be published in Clay and Clay Minerals.
8. W. Kundig, J.A. Cape, R.H. Lindquist, G. Constabaris,J. Appl. Phys. 38, 947 (1967).
9. V.U.S. Rao, F.E. Huggins and G.P. Huffman, J.Appl.Phys. 50, 2048 (1979).
10. R.P. Blakemore, D. Maratea and R.S. Wolfe, J.Bacterio. 140, 720 (1979).
11. D.L. Balkwill, D. Maratea and R.P. Blakemore, J.Bacteriol. 141, 1399 (1980).
12. R.B. Frankel, R.P. Blakemore and R.S. Wolfe, Science 203, 1355 (1979).
13. R.B. Frankel, R.P. Blakemore, J. Magn. and Magn.Maters. 15, 1562 (1980).
14. R.P. Blakemore and R.B. Frankel, Sci. Am. 245, 58 (1981)
15. R.P. Blakemore, R.B. Frankel and A.J. Kalmijn, Nature (London), 286, 384 (1981).
16. R.B. Frankel, R.P. Blakemore, F.F. Torres de Araujo, D.M.S. Esquivel , J. Danon, Science, 212, 1269 (1981).
17. D.M.S. Esquivel, H.G.P.Lins de Barros, M. Farina, P.H. A. Aragão, J. Danon, Biol. Cell. 47, 227 (1983).
18. R.B. Frankel, G.C. Papaefthymiou, R.P. Blakemore, W.D. O'Brien, Biochim. Biophys. Acta (in press).
19. A. Blaise, J. Chappert, J.L. Giradet, C.R. Acad. Sci. Paris, 261, 2310 (1965).

20. E.R. Bauminger, S.G. Cohen, D.P.E. Dickson, A. Levy, S. Ofer, J. Yariv, Acta 623, 237 (1980).
21. G.A. Clegg, J.E. Fitton, P.M. Harrison, A. Treffery, Prog. Biophys. Molec. Biol. 36, 56 (1980).
22. S. Ofer, I. Nowik, E.R. Bauminger, G.C. Papaefthymiou, R.B. Frankel, R.P. Blakemore, Biophys. J. (submitted).
23. P.P. Craig, N. Suttin, Phys. Rev. Lett. 11, 460 (1983).
24. E.R. Bauminger, S.G.Cohen, S. Ofer, U. Bachrach, Biochim. Biophys. Acta 720, 133 (1982).
25. E.R. Bauminger, S.G. Cohen, I. Nowik, S. Ofer, J.Yariv, Proc. Natl. Acad. Sci. (USA) 80, 736 (1980).
26. I. Nowik, S.G. Cohen, E.R. Bauminger, S. Ofer, Phys.Rev. Lett. 50, 1528 (1983).
27. J. Wood, Meteorites and the Origin of Planets, McGraw-Hill Inc. 1968.
28. J.F. Albertsen, M. Aydin, J.M. Knudsen, Phys. Scripta 17, 467 (1978).
29. J.F. Albertsen, G.B. Jensen, J.M. Knudsen, J. Danon, Meteoritics 13, 379 (1978).
30. J. Danon, R.B.Scorzelli, I. Souza Azevedo, M.Christophe-Michel-Levy, Nature 281, 469 (1979).
31. J.F. Albertsen, N.O. Roy-Poulsen, L. Vistisen, Meteoritics, 15, 258 (1980).
32. J.F. Albertsen, Thesis, University of Copenhagen (1981).
33. J.Paulevē, D. Dautreppe, J. Laugier, L. Nēel, C.R.Acad. Sci. Paris 254, 965 (1962).
34. Y. Gros, J. Paulevē, J. Physique 31, 459 (1970).
35. J.F. Albertsen, Phys. Scripta 23, 301 (1981).
36. E.R.D. Scott, R.S. Clarke, Nature 281, 532 (1979).
37. L. Larsen, H. Roy-Poulsen, N.O. Roy-Poulsen, L. Vistinen, J.M. Knudsen, Phys. Rev. Letters 48, 1054 (1982).
38. J.Danon, I. Souza Azevedo, R.B.Scorzelli, Meteoritics, 17, 202 (1982).

FIGURE CAPTIONS

Fig. 1 - Fragments of the structure of sheet silicates. a) 1:1 layer and b) 2:1 layer.

Fig. 2 - Magnetic hyperfine spectra at 4.2K; a) greenalite, b) cronstedtite, c) minnesotaite, d) ferripyrophyllite, e) crocidolite, f) ilvaite. All are powder samples.

Fig. 3 - Schematic magnetic structure for greenalite determined by neutron diffraction.

Fig. 4 - a) Antiferromagnetic order in an hexagonal lattice, b) Frustration in a triangular lattice.

Fig. 5 - Schematic magnetic structure for crocidalite.

Fig. 6 - Mössbauer spectrum of wet packed magnetotactic bacteria (MS-1) at 200K. Spectrum A is due to Fe_3O_4 ; spectrum B is a ferric doublet; spectrum C is a ferrous doublet.

Fig. 7 - Mössbauer spectrum of lyophilized non-magnetotactic cells. a) 100K; b) 40K; c) 4.2K.

Fig. 8 - Mössbauer spectrum of wet, packed cells of a non-magnetotactic strain at a) 4.2K and b) in a longitudinal magnetic field of 60 kOe.

Fig. 9 - Mössbauer spectra of taenite from meteorites. a) Toluca, b) Santa Catharina and c) Saint Séverin.

Fig. 10 - Mössbauer parameters of tetrataenite for different iron meteorites. The internal field H_i and the quadrupole splitting ΔE vary with the degree of order of tetrataenite. The state of order reflets the different cooling experienced by the meteorites below the transition temperature T_c = 320ºC.

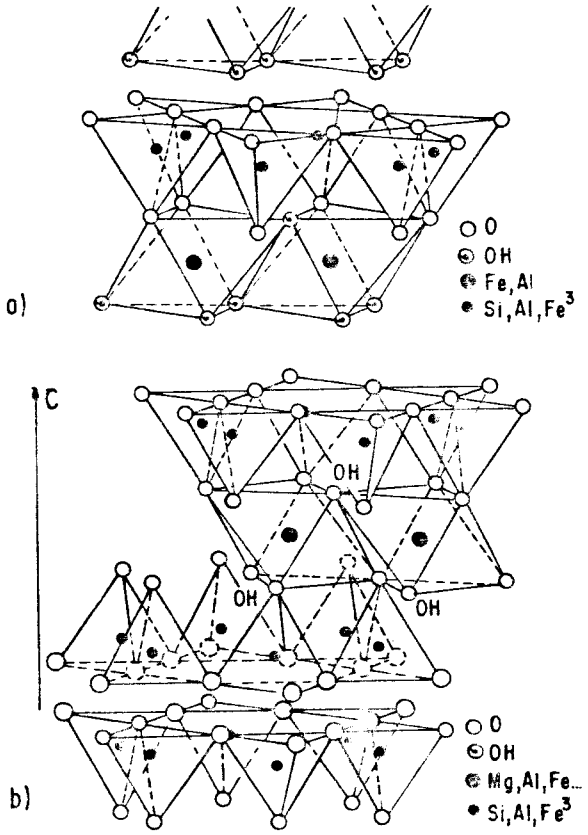

FIG.1

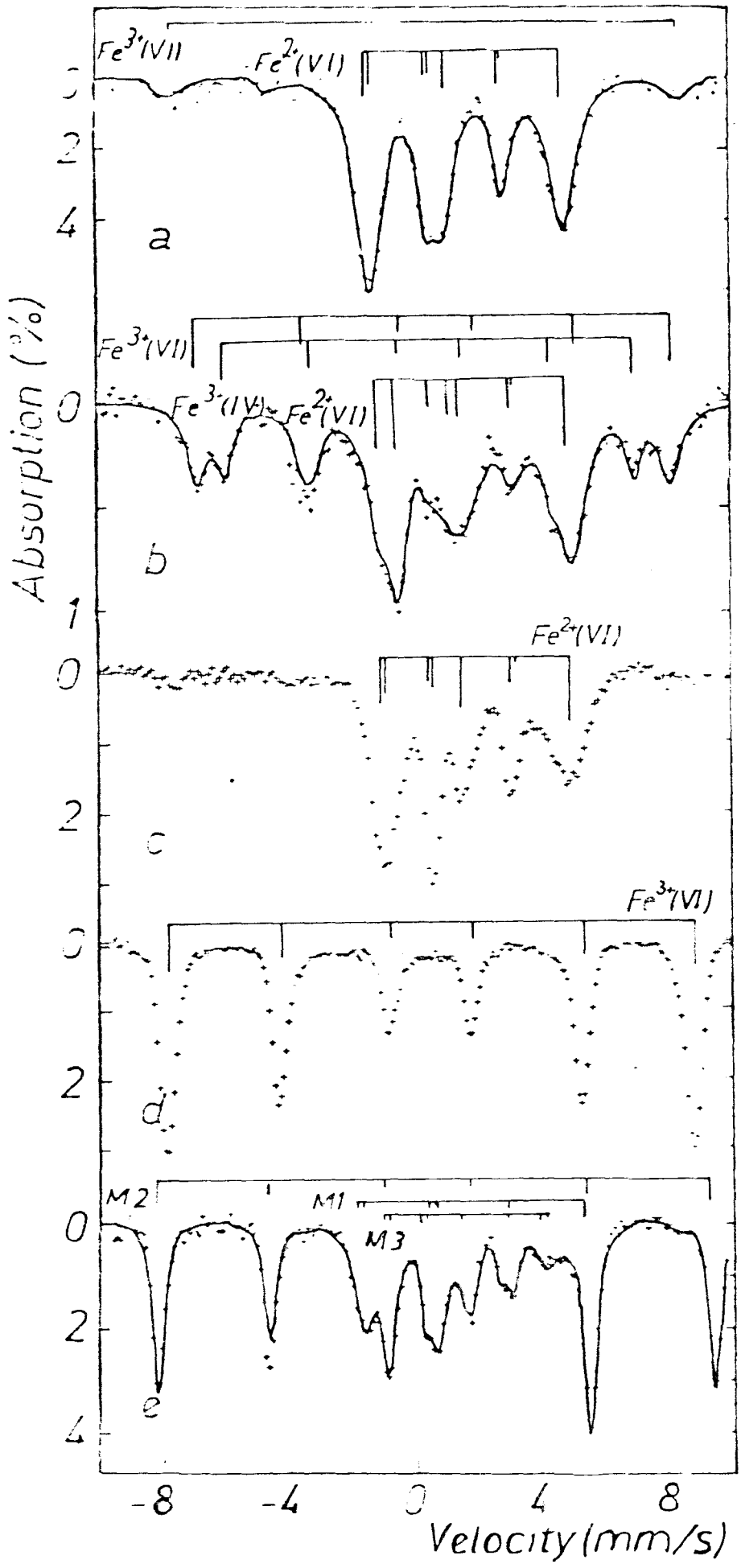
Fe3+(VII)
Fe2+(VI)
a
Fe3+(VII)
Fe3+(IV)
Fe2+(VII)
b
Fe2+(VII)
c
Fe3+(VI)
d
M2
M1
M3
e
Absorption (%)
-8
-4
0
4
8
Velocity (mm/s)

FIG.2

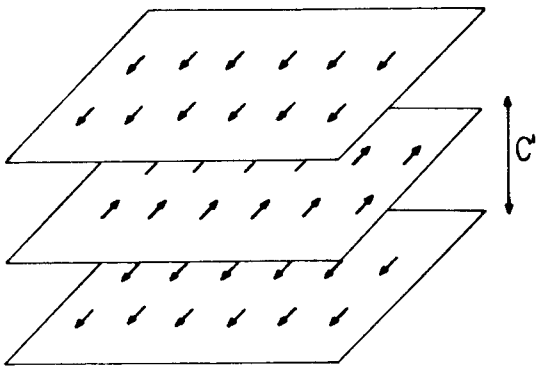

FIG.3

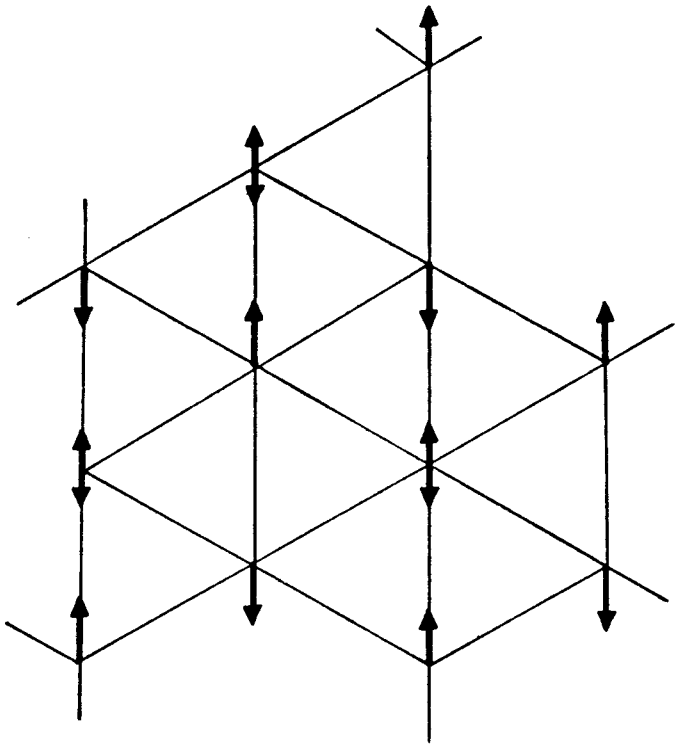

4b

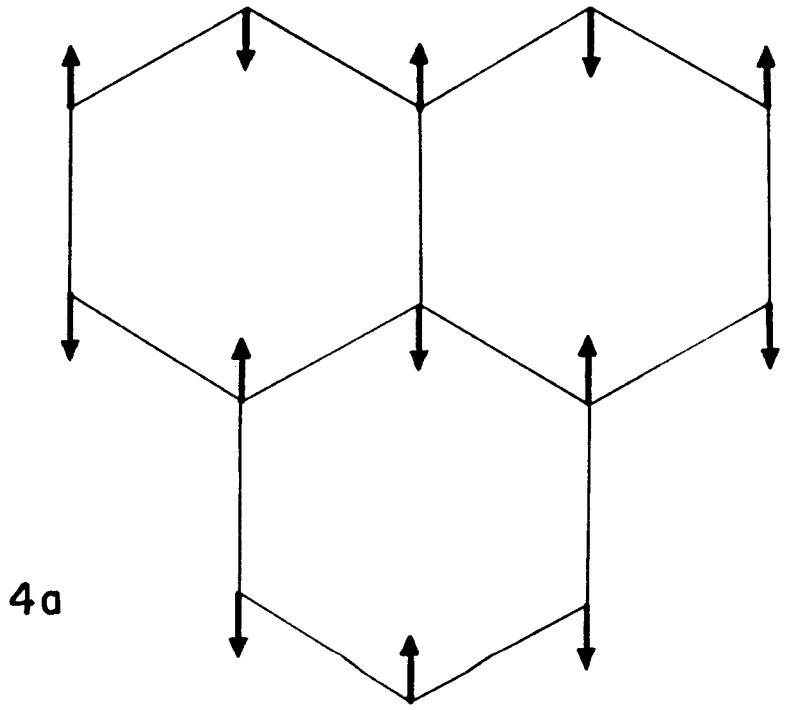

4a

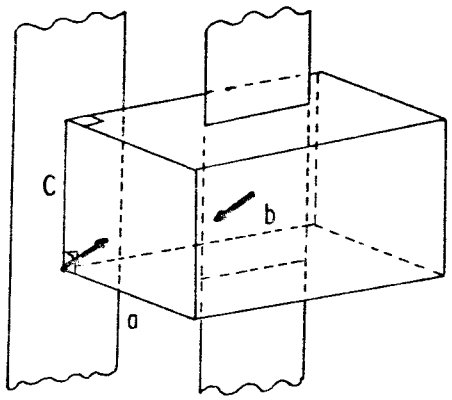

FIG.5

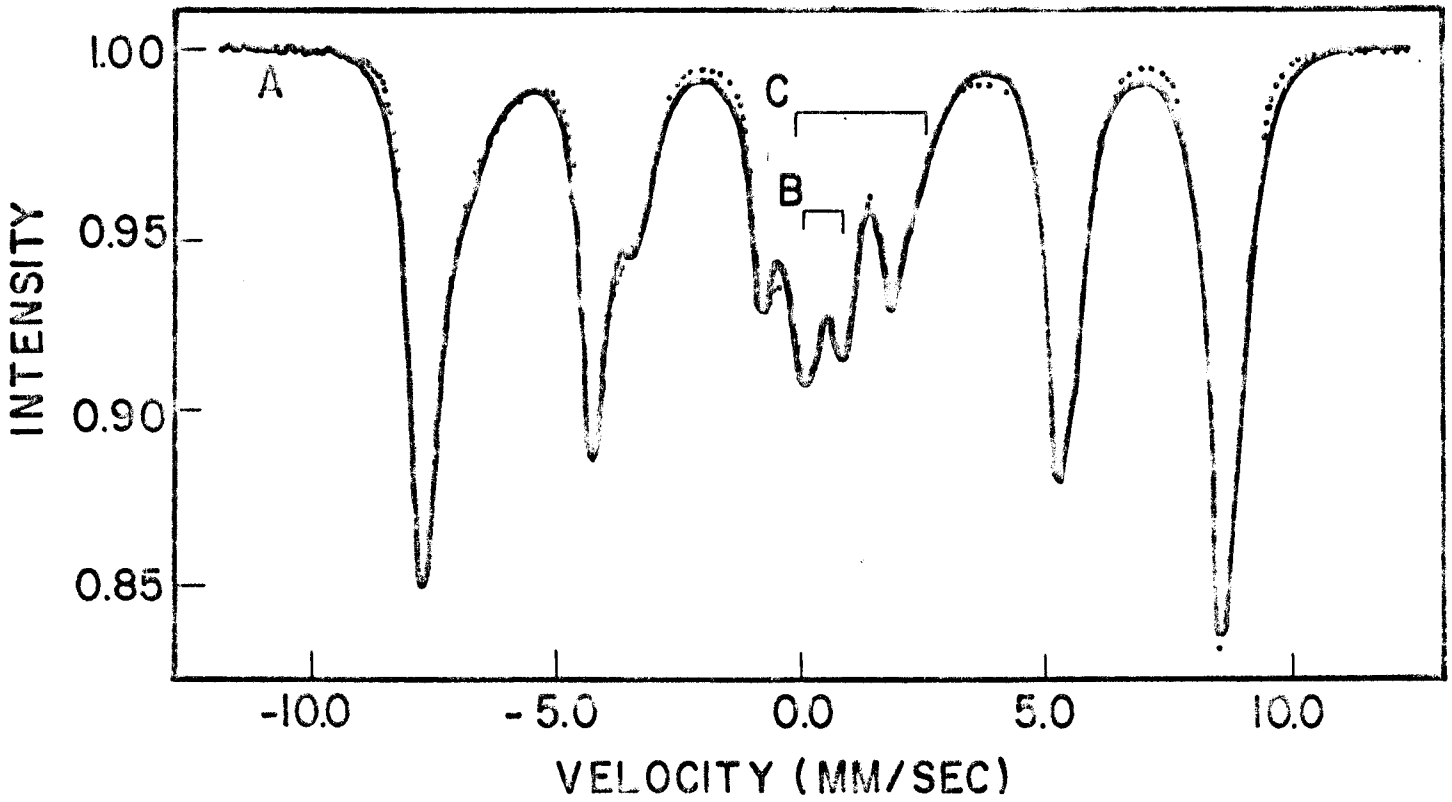

FIG. 6

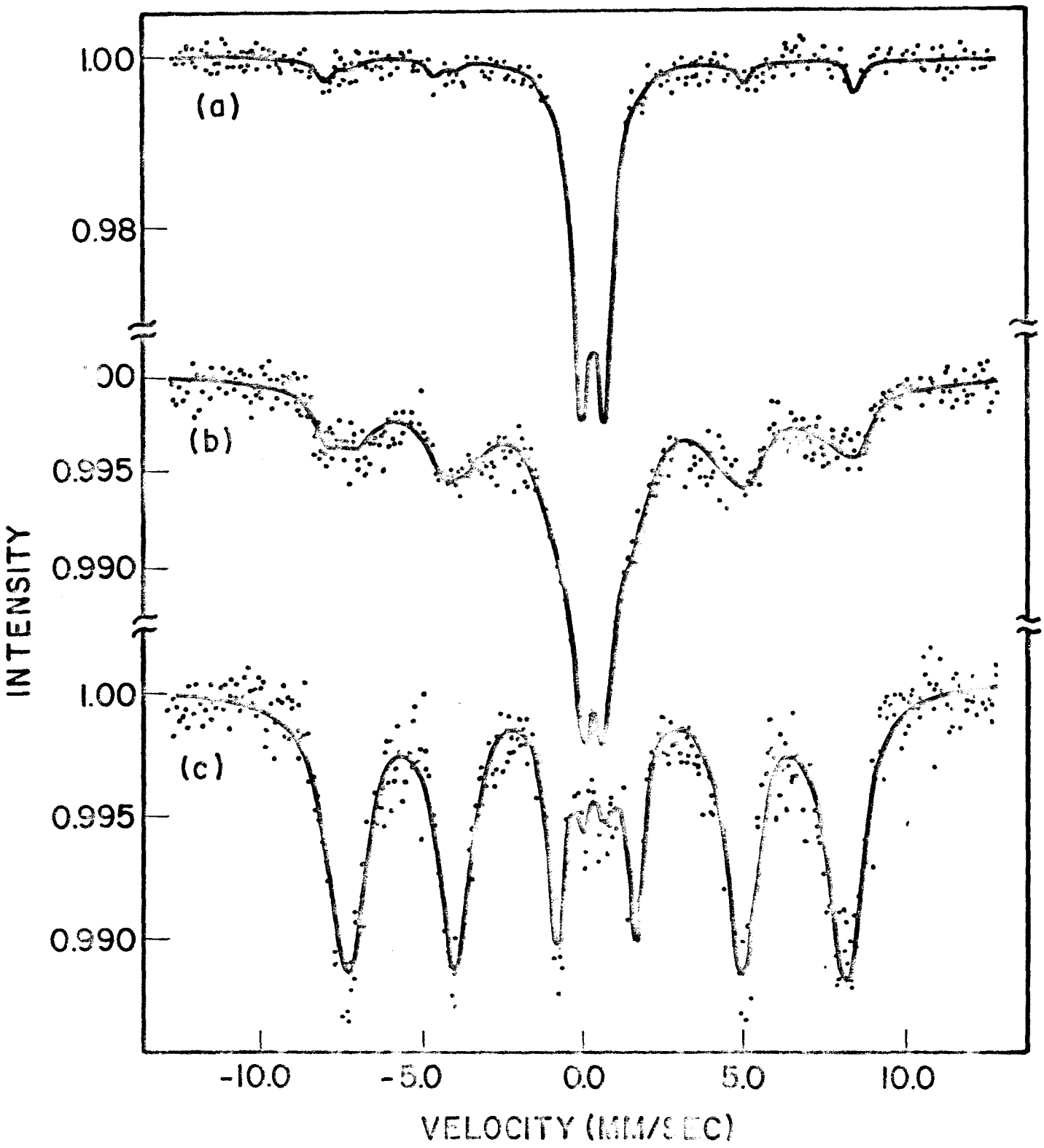
1.00
(a)
0.98
00
(b)
0.995
0.990
1.00
(c)
0.995
0.990
INTENSITY
-10.0
-5.0
0.0
5.0
10.0
VELOCITY (MM/SEC)

FIG. 7

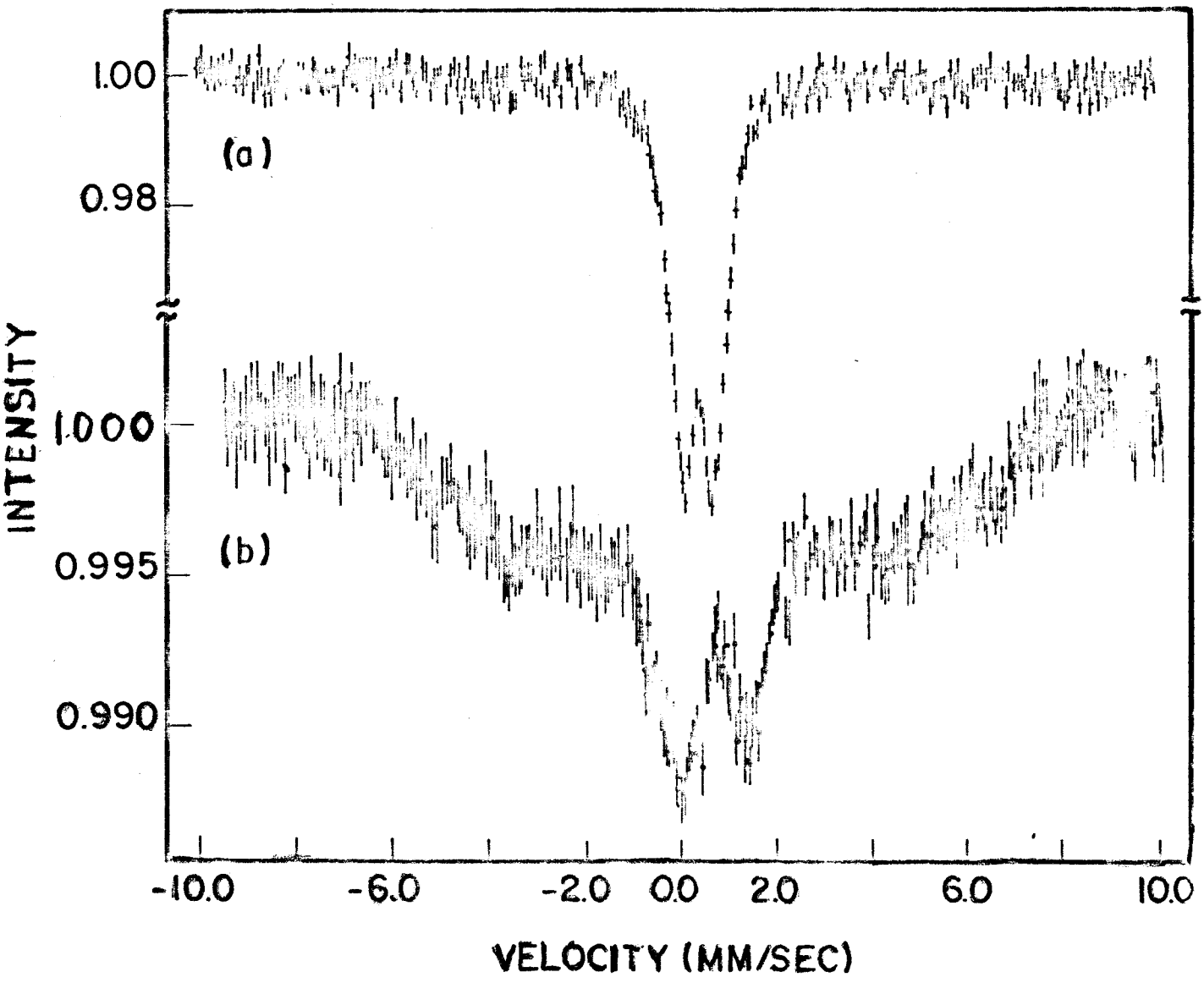
1.00
0.98
1.000
0.995
0.990
INTENSITY
(a)
(b)
-10.0
-6.0
-2.0
0.0
2.0
6.0
10.0
VELOCITY (MM/SEC)

FIG.8

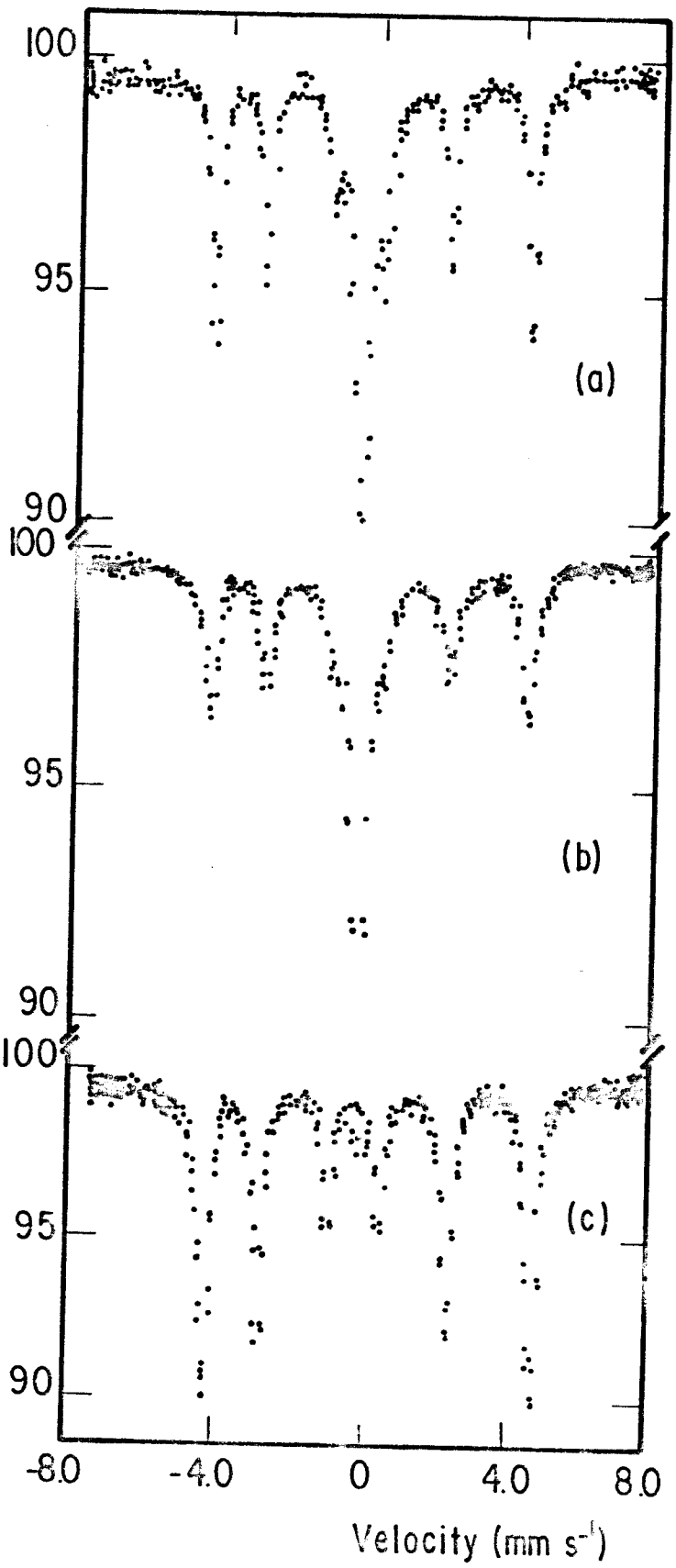

FIG. 9

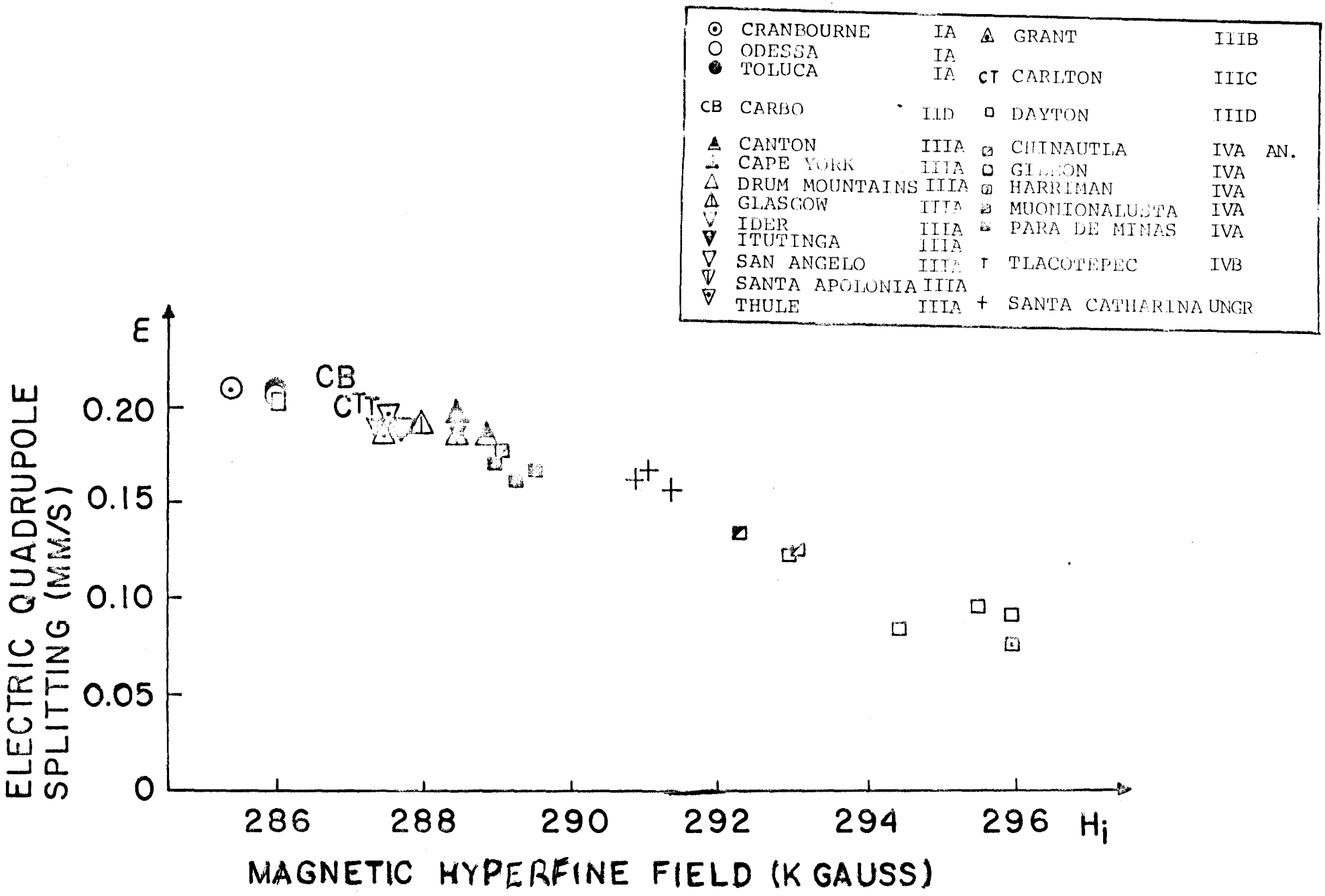
CRANBOURNE IA
ODESSA IA
TOLUCA IA
CB CARBO IID
CANTON IIIA
CAPE YORK IIIA
DRUM MOUNTAINS IIIA
GLASGOW IIIA
IDER IIIA
ITUTINGA IIIA
SAN ANGELO IIIA
SANTA APOLONIA IIIA
THULE IIIA
GRANT IIIB
CT CARLTON IIIC
DAYTON IIID
CHINAUTLA IVA AN.
GI[illegible]ON IVA
HARRIMAN IVA
MUONIONALUSTA IVA
PARA DE MINAS IVA
TLACOTEPEC IVB
SANTA CATHARINA UNGR
ε
CB
CT
0.20
0.15
0.10
0.05
0
286
288
290
292
294
296
Hi
ELECTRIC QUADRUPOLE SPLITTING (MM/S)
MAGNETIC HYPERFINE FIELD (K GAUSS)

FIG. 10

TABLE

MAGNETIC ORDERING TEMPERATURES FOR IRON-RICH SILICATE MINERALS

	T_N (K)		T_N (K)
1:1 layer silicates		Amphiboles	
Greenalite	17	Grunerite	45
Berthierine	9	Riebeckite	23
Cronstedtite	12	Crocidolite	30
2:1 layer silicates		Group silicates	
Ferripyrophyllite	18		
Minnesotaite	20	Fayalite	66
Glauconite	∿4	Laihunite	∿80
Montronite	2	Staurolite	6
Biotite	7		
Thuringite	∿4		
Pyroxenes		Ilvaite	90
Orthoferrosilite	37		